J Inorg Organomet Polym (2013) 23:1240–1246
DOI 10.1007/s10904-013-9915-9

Coordination Self-Assembly of Heterogenite Nanosheets into Uniform Nanospheres Through an Ultrasonic-Assisted Process

Jing Yang · Lishuang Yao · Jingwei Sun · Bo sun

Received: 24 May 2013 / Accepted: 17 July 2013 / Published online: 26 July 2013

Abstract Large-scale uniform β-CoOOH nanospheres were prepared under ultrasonic conditions through coordination self-assembly of heterogenite nanosheets. The nanospheres were composed of about 10 nm-thick single-crystalline nanosheets with the averaged diameter of about 120 nm. A rational mechanism based on the coordination self-assembly and oriented attachment through ultrasonic assisted process is proposed for the self-assembly of heterogenite single-crystal nanosheets into nanospheres. This result may facilitate not only the exploration of the preparation of the heterogenite nanostructures through a simple and facile controlled-route, but also a general approach for the large-scale, high-purity growth of different nanostructures of a wide range of transition metal correlated materials.

Keywords Nanosphere · Nanosheet · Heterogenite · Ultrasonic

1 Introduction

Over the past several years, large-scale mesoscale assembly of one or multidimensional nanostructured building blocks into ordered structures has attracted significant interest in materials synthesis and device fabrications [1–10]. In addition to one-dimensional (1D) or two-dimensional (2D) assembled structures, much effort has been focused on fabricating curved structures such as spherical and tubular structures [11–15]. These ordered nanospheres are expected to have potential applications in catalysts, drug carriers, and magnetic recording due to their dimensions and high surface areas [14–17]. The ability to synthesize uniform nanospheres with diameters ranging from nano- to micro-scale sizes is desirable. Regarding generation of curved architectures from prefabricated components, two general synthesis strategies have been employed for "bottom-up" chemical synthesis: (i) the use of various templates, which physically confine the shape of nanostructures (such as droplets, silica, and block copolymers [18–21]); and (ii) the use of interaction among nanostructure-units, which self-assembles artificial building blocks (i.e., 1D organic–inorganic hybrid rods) into various curved single-layer superstructures [22]. These assembled structures, however, are apt to fragmentate under the exoteric disturbance due to the weak mutual bond among the units. Here, we report a new kind of strong bond to generate the curved architectures via coordination self-assembly.

Heterogenite has a brucite-like structure constructed of layers of edge-sharing Co^{3+} oxohydroxo octahedral (see Fig. 1a). Recently heterogenite (β-CoOOH) has attracted renewed and growing interest in the field of the electrode materials because of the excellent conductivity [23–26]. As is well known, cobalt oxide is an indispensable component in the positive electrodes of rechargeable alkaline nickel-based batteries to achieve high electrochemical efficiency. Whether it is cobalt, cobalt oxide, or cobalt hydroxide, however, they are finally converted into CoOOH, which

J. Yang · B. sun (✉)
School of Pharmaceutical Sciences, Changchun University of Chinese Medicine, 1035 Boshuo Road, Jingyue Economic Development District, Changchun 130117, People's Republic of China
e-mail: sunbowulihuaxue@126.com

L. Yao · J. Sun
Changchun Institute of Optics, Fine Mechanics and Physics, Chinese Academy of Sciences, Changchun 130033, People's Republic of China

can obviously improve the charge efficiency and cycling stability in nickel-metal hydride (Ni-MH) cells owing to the higher conductivity phase of the formed CoOOH than NiOOH. Currently the reported study on heterogenite only limited their bulks [27]. However, it was found that for an electric material, controlling its mesoscale size and shape is of crucial importance to the study of its electric property. So it is a challenge to prepare heterogenite at the nanometer scale. Here we report on the synthesis of β-CoOOH curved nanostructures composed of nanosheets under ultrasonic conditions.

The general synthesis of β-CoOOH is based on the reaction of Co^{2+} cations and an oxidant, such as the oxidation of β-$Co(OH)_2$ [28] and one-step synthesis of cobalt salt in alkaline conditions with different oxidants, such as O_2 [29] and H_2O_2 [30]. While in this paper, we report a novel synthesis route to the formation of β-CoOOH, which is the direct hydrolysate of Co^{3+} simple complex, $[Co(NH_3)_5(H_2O)]Cl_3$. As is well known, Co^{2+}/Co^{3+} cations can coordinate with the ammonia to form the cobaltammines with different coordination structures, such as $[Co(NH_3)_4]Cl_2$, $[Co(NH_3)_6]Cl_3$, $[Co(NH_3)_5Cl]Cl_2$, and so on. The different hydrolysates of the cobaltammines precursors could offer a scheme to synthesize different assemblies of cobalt oxide, hydroxide and oxyhydroxide, which are of crucial importance to the study of their property.

2 Experimental Section

2.1 Materials

All chemicals were analytical grade and were used without further purification. Hydrochloric acid (HCl, 36–38 %), ammonia ($NH_3 \cdot H_2O$, 60 %), hydrogen peroxide (H_2O_2, 30 %), cobaltous chloride ($CoCl_2 \cdot 6H_2O$) and ammonium chloride (NH_4Cl) were purchased from Beijing Chemical Reagent Co. Ltd. of China. Deionized water was prepared in our laboratory.

2.2 Synthesis of the β-CoOOH Nanosphere

The $[Co(NH_3)_5(H_2O)]Cl_3$ precursor was dissolved in water to obtain 0.01, 0.02 and 0.04 M solution. The resulting aqueous solution was kept at 50 °C for 8 h under ultrasonic conditions with a frequency of 40 kHz and a nominal power 250 W, and then cooled to room temperature naturally. The obtained blue product was filtered and washed several times with distilled water and absolute ethanol, and finally dried in a vacuum oven at 60 °C for 12 h.

2.3 Characterization

The X-ray powder diffraction (XRD) patterns of the products were measured on a Rigaku X-ray diffractometer with Cu Kα radiation (λ = 1.5418 Å) in the 2θ range of 15°–100°. Field-emission scanning electron microscope (FE-SEM) was performed with a JEOL-7500B microscope operated at an acceleration voltage of 10 kV, and transmission electron microscopy (TEM) was carried out on the Hitachi H-800 TEM. High-resolution transmission electron microscopy (HRTEM) images were obtained using a JEOL-2010 TEM at an acceleration voltage of 200 kV. Fabrication and analysis of gas sensors were performed according to the reported literature [31].

3 Results and Discussion

The phase composition of the as-obtained sample was examined by XRD. As shown in Fig. 1b, all of the peaks can be perfectly indexed to a pure rhombohedral phase (space group: $R^{-}3m$ [166]) of β-CoOOH with lattice constants a = 2.855 Å and c = 13.156 Å (JCPDS card No 07-0169), and no other impurities have been observed in

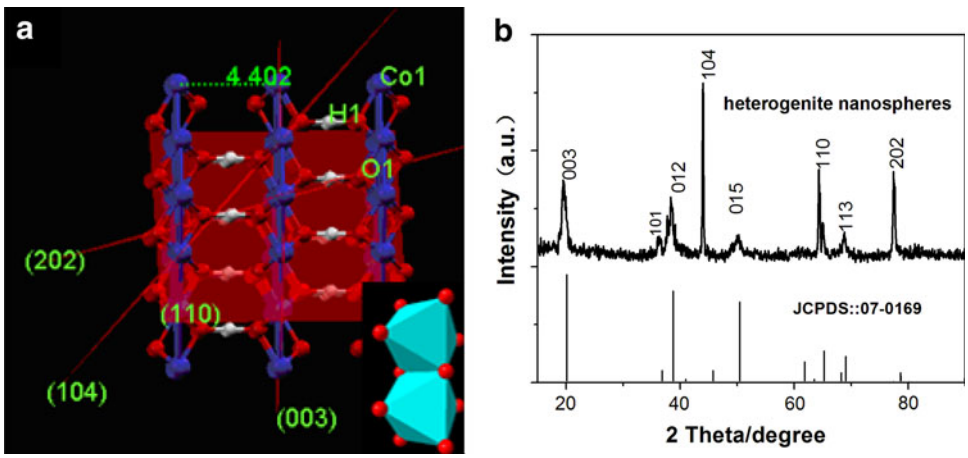

Fig. 1 **a** Schematic crystalline structures of heterogenite. **b** X-ray diffraction (XRD) pattern of the as-synthesized nanospheres assembled with nanosheets

the synthesized product. In addition, it was found that (104) and (202) peaks gained a substantial increase in relative intensity, indicating that the nanomaterial growth might occur along the ⟨104⟩ and ⟨202⟩ directions. So, from the β-CoOOH crystal structure (Fig. 1a), we can suppose that the product may have an intersectant-layer structure.

The morphology of the as-synthesized product was examined by the TEM and the FE-SEM. Figure 2a, b show the FE-SEM images of the same sample. Figure 2a is a lower magnification view of the product, indicating the primary morphology of uniform nanospheres. Figure 2b shows an SEM image at a higher magnification, from which it can be seen that the nanosphere is composed of about 10 nm-thick nanosheets with the averaged diameter of about 120 nm. The TEM image in Fig. 2c shows that the spheres have sheet-interlaced structures with a diameter of ∼120 nm, consistent with the size observed by SEM. The selected-area electron diffraction (SAED) pattern, as shown in Fig. 3d exhibits that the nanospheres have a polycrystalline structure with a good crystallinity. As is interested, there are some semblable sandwiches of β-CoOOH nanoassemblies (as is shown in Fig. 2b with the arrow) with the lamellar spacing of several nanometers, which may offer a new type of the host nanomaterials where the guest of nanoscale $Ni(OH)_2$ inserts for Ni-MH cells. Further studies on the applications of β-CoOOH nanospheres as a kind of host material are still in progress.

Further structural characterization of nanospheres was carried out by high-resolution TEM (HRTEM). Figure 3a, b show HRTEM images taken from the areas at the face and the edge of the nanosheets within the same nanosphere. The HRTEM image (Fig. 3a) suggests that the calculated interface fringe spacing is about 4.4 Å, which corresponds to the (003) plane of rhombohedral β-CoOOH (Fig. 1a), and the nanosheets are slight polycrystalline sheets consisting of β-CoOOH nanocrystallites indicated by the arrows. However, the fast Fourier transform (FFT) of HTEM pattern (Fig. 3c) corresponding to the selected area (see the rectangular dashed-line boxes in Fig. 3a) shows the well-recorded pattern which implies that the individual nanosheet is a single crystal, but the surfaces are partially covered with a small quantity of nanocrystals that mask the single crystalline structure of the nanosheet core, which is similar with $Cu(OH)_2$ nanoribbons obtained by the coordination self-assembly mechanism [32]. Furthermore, the well-recorded FFT pattern also suggests that orientations of the crystallites are not random but coordinated with the [003] direction being the preferential growth direction of the single-crystalline nanosheets. Meanwhile, the HRTEM image (Fig. 3b) in the edge of the nanosheet shows a crystalline character with a lattice spacing of 4.4 Å, which can also be indexed to the (003) plane of rhombohedral rhomb-centered β-CoOOH, and the thickness of ∼10 nm, consistent with the size observed by SEM. The FFT of HTEM pattern (Fig. 4d) corresponding to the selected area (see the rectangular dashed-line boxes in Fig. 3b) shows that the products exhibit a single-crystal structure. So, we can consider that the nanosheets possess single-crystalline structure.

The concentration of $[Co(NH_3)_5(H_2O)]Cl_3$ significantly affects the morphology and size of the product. The higher the concentration of $[Co(NH_3)_5(H_2O)]Cl_3$ is, the more the nanosheet branches of the nanospheres are. For example, when the concentration of $[Co(NH_3)_5(H_2O)]Cl_3$ was increased from 0.01 to 0.04 M while maintaining a constant reaction temperature of 50 °C, the amount of the nanosheets, of which the nanospheres consist, obviously increases (Fig. 4a, b), somewhat similar to CuO dandelions in the shape [33], and the size of the nanospheres on the average diameter varies from 120 nm at 0.01 M (Fig. 2b), to 150 nm at 0.02 M (Fig. 4c), and yet 70 nm at 0.04 M (Fig. 4d). These results suggest that it is possible to control and tune the shape β-CoOOH spherical nanostructures by controlling the reactant concentration, that is, the kinetic parameters of the crystal growth crystal orientations.

Heterogenite (β-CoOOH) has a layer-like structure, which tends to grow along the layer and form sheet-like products [27, 34]. In our case, we believe that β-CoOOH formation proceeds two steps (Eq. (1)) under ultrasonic conditions: first, $[Co(NH_3)_5(H_2O)]^{3+}$ ions quickly convert to $[Co(OH)_5(H_2O)]^{2-}$ via the substitution reaction between NH_3 and OH^-; second, the $[Co(OH)_5(H_2O)]^{2-}$ ions are further transformed to β-CoOOH via the dehydration-condensation reaction among OH^- and H_2O.

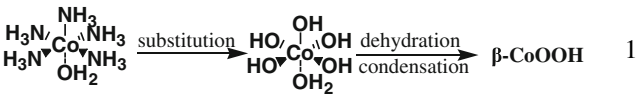

(1)

From the structural characteristics, $[Co(NH_3)_5(H_2O)]^{3+}$ and $[Co(OH)_5(H_2O)]^{2-}$ both have a distorted octahedral structure, which may cause the product growth along different orientations. In previous research, although many other routes through the coordination self-assembly mechanism were developed to prepare $Cu(OH)_2$ nanomaterials [32, 35], no oriented alignment of 2D objects has been observed. As we know, β-CoOOH and $Cu(OH)_2$, which both are the layered materials, have a similar structure. However, $[Cu(NH_3)_4]^{2+}$, which has a panel structure, leads to a 1D $Cu(OH)_2$ nanostructures. Further, at the same synthesized condition, we find that the reactive product of $[Co(NH_3)_5Cl]Cl_2$ is also constructed spherical assemblies of β-CoOOH (Fig. 5), which is similar with that of $[Co(NH_3)_5(H_2O)]Cl_3$, but the solution of $[Co(NH_3)_6]Cl_3$

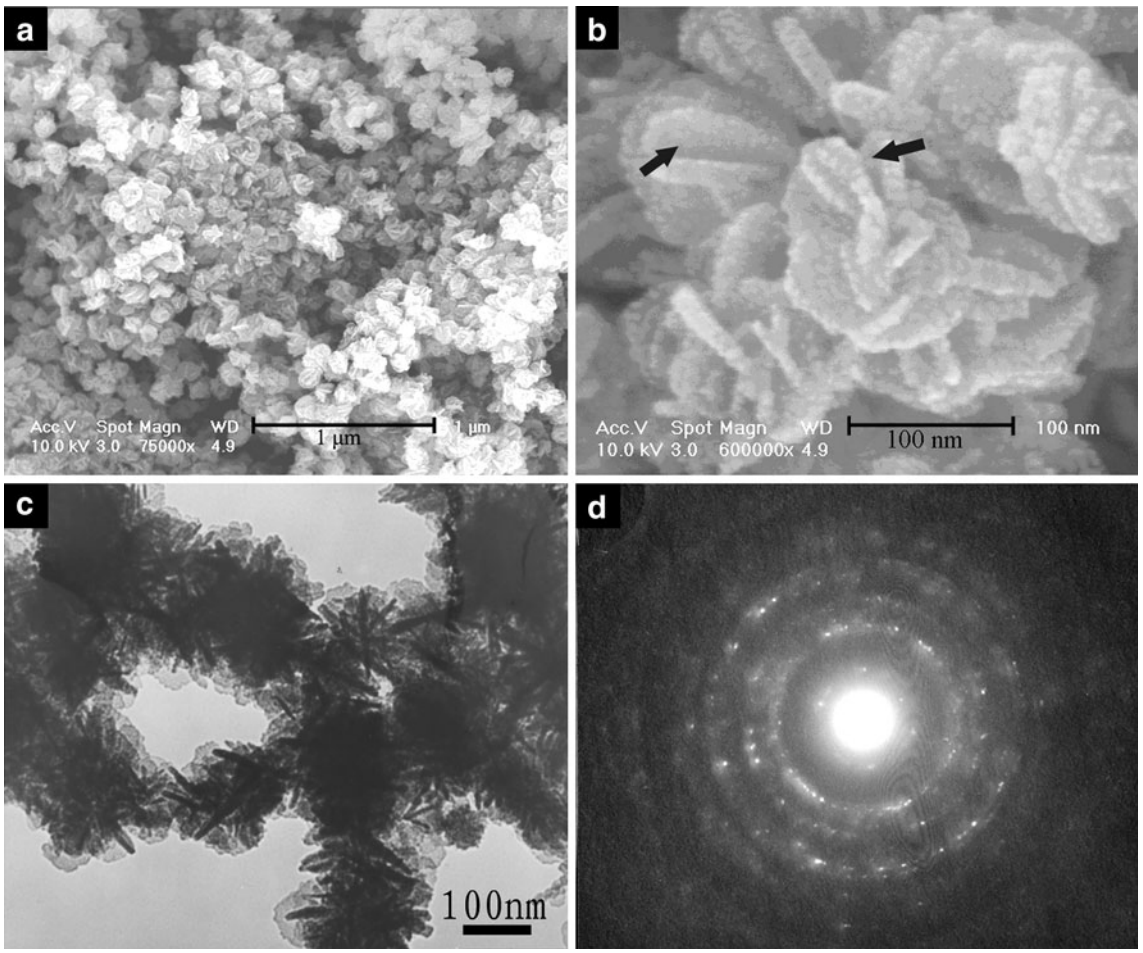

Fig. 2 **a** Low-magnification, **b** high-magnification FE-SEM and **c** TEM image of β-CoOOH nanospheres; **d** the SAED image of the nanospheres

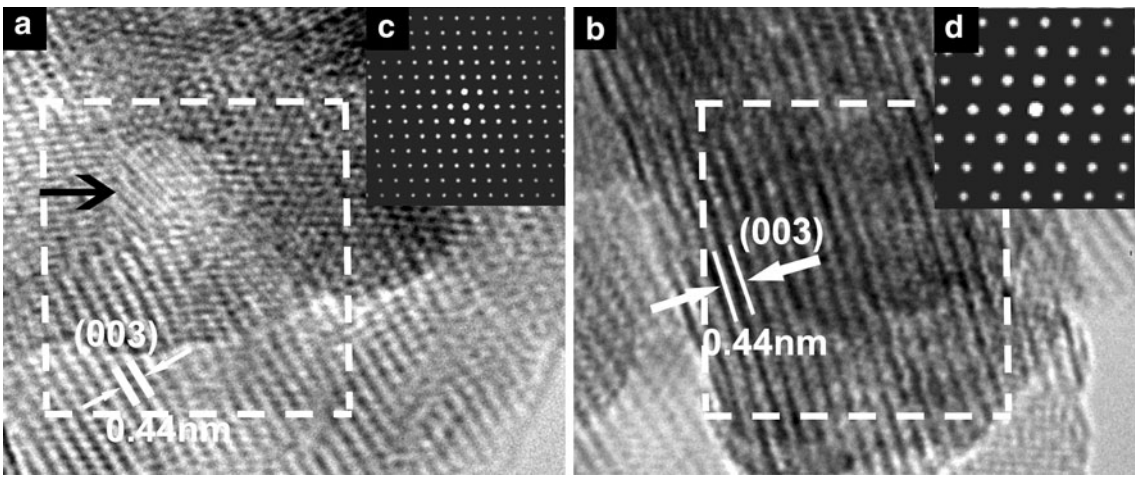

Fig. 3 HRTEM image of β-CoOOH nanosheets for the face (**a**) and the edge (**b**); The FFT of HRTEM images (*c* and *d*) recorded from the rectangles enclosed areas in (**a**) and (**b**) respectively

is not obviously changed. We think that the distorted octahedral coordination structures of $[Co(NH_3)_5(H_2O)]Cl_3$/$[Co(NH_3)_5Cl]Cl_2$ are more apt to promote the reaction than the regular octahedral coordination structure of $[Co(NH_3)_6]Cl_3$. Therefore, in the current work, the precursor of $[Co(NH_3)_5(H_2O)]^{3+}$, which has the distorted

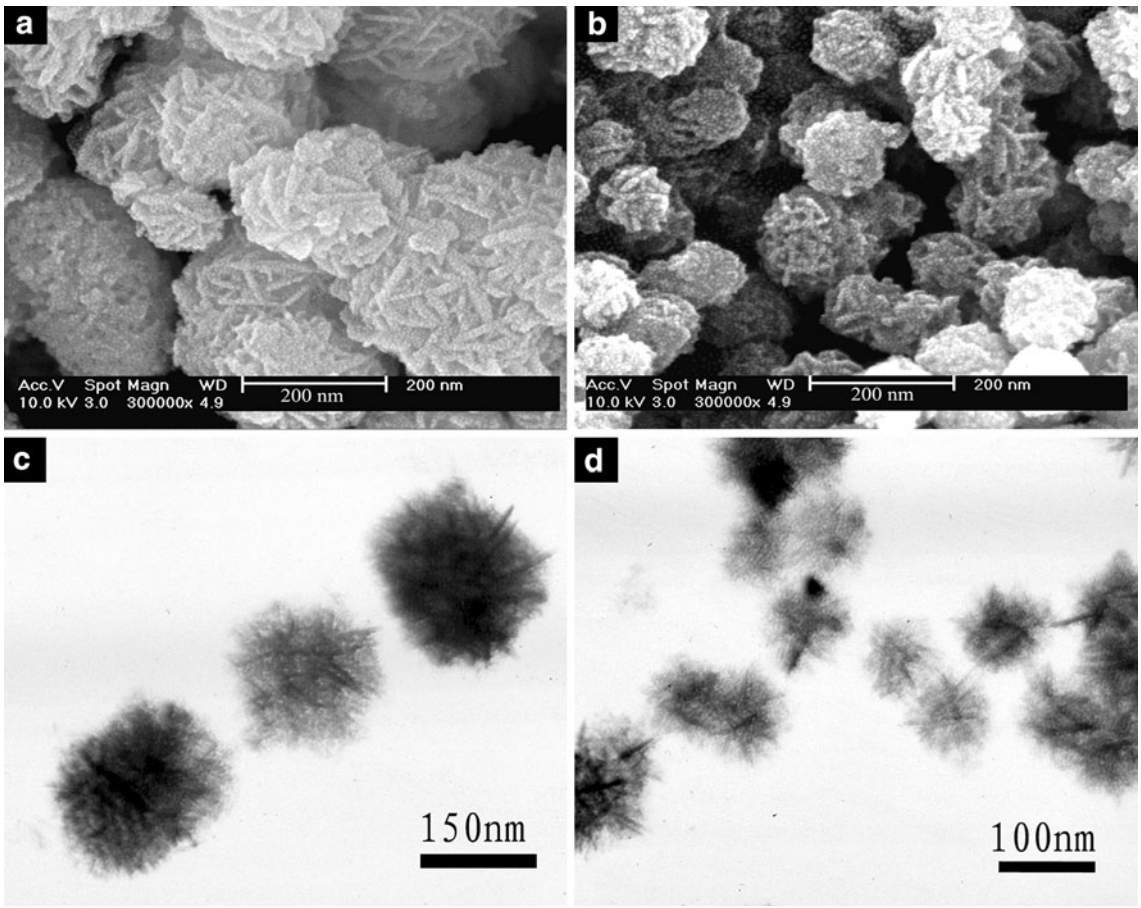

Fig. 4 SEM and TEM images of synthesized products at different conditions: 0.02 M (**a**, **c**) and 0.04 M (**b**, **d**)

octahedral coordination structures between the metal ions and ammonias, is undoubtedly vital to the formation of the spherical assembly.

The ultrasonic irradiation offers a kinetic process different from other processes such as hydrothermal, and can promise a very short reaction time and relatively stable reaction conditions, which come from the enhanced Ostwald ripening processes [36, 37]. So, the ultrasonic assisted process often leads to more uniform nanostructures [37, 38], which is also one of the main reasons why large-scale, uniform β-CoOOH nanospheres were prepared in the current case.

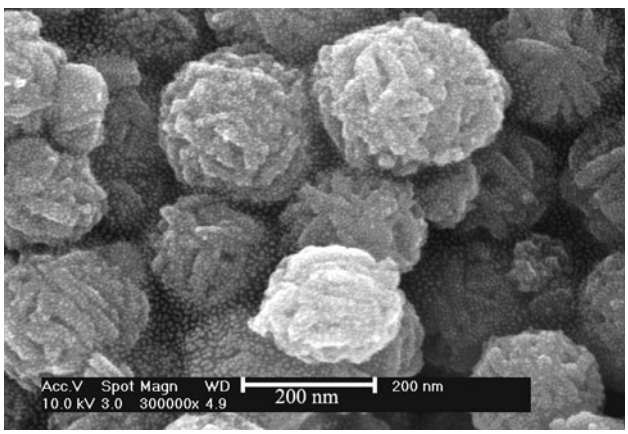

Fig. 5 SEM of synthesized products of $[Co(NH_3)Cl]Cl_2$ at the same condition of $[Co(NH_3)H_2O]Cl_3$: 0.01 M, 50 °C, 8 h

For the formation of β-CoOOH spherical assemblies, a coordination self-assembly mechanism, inspired by a promising recent study on the formation of $Cu(OH)_2$ 1D nanostructures [37], is proposed based on heterogenite crystalline structure (Fig. 1a) and the HRTEM images at the face and the edge of the nanosheets within the same nanosphere. During the synthesis of the β-CoOOH nanospheres, the nanosheets form as nuclei, which grow along [001] direction (c axis) because of the selective dehydration-condensation from OH^- that are coordinated with Co^{3+} ions in the square planar way, resulting in the increase of OH^- in the face of nanosheets (Step 1 in the Scheme 1). Subsequently, when OH^- in the face of nanosheets is condensed with OH^- of $[Co(OH)_5(H_2O)]^{2-}$, the growth along $\langle 104\rangle/\langle 202\rangle$ takes place parallel to the (003) plane, which causes intersectant nanosheets to self-assemble nanospheres through the strong function of Co–O

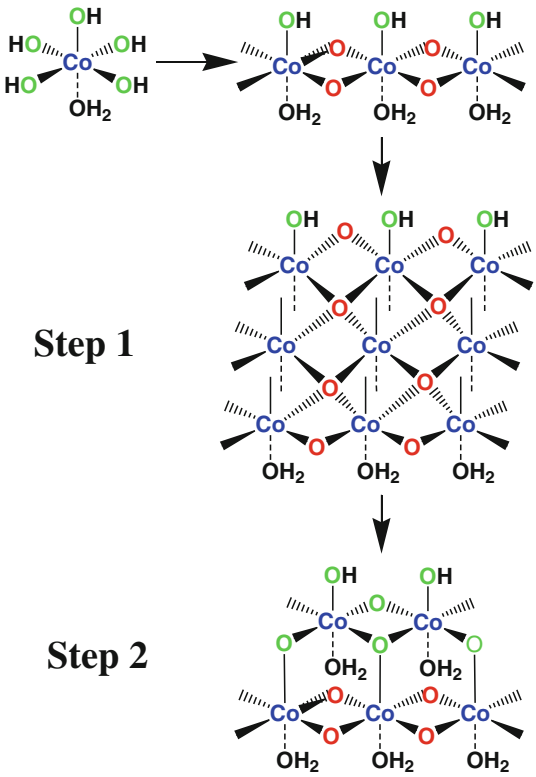

Scheme 1 Schematic showing the coordination assembly growth of β-CoOOH nanospheres composed of nanosheets

covalent bond (Step 2 in the Scheme 1). Further, with the increase of the $[Co(NH_3)_5(H_2O)]^{3+}$ precursor, the whole reaction speeds up and the reaction rates of the second step at different directions become faster than the growth rate of the sheet, namely the crystal orientations. So, it causes to more branches within the nanosphere.

4 Conclusion

In summary, we have successfully synthesized large-scale uniform β-CoOOH nanospheres via coordination self-assembly of heterogenite nanosheets by an ultrasonic-assisted process. The concentration of the cobaltammine precursor $[Co(NH_3)_5(H_2O)]Cl_3$ could affect β-CoOOH size and morphology. The nanospheres synthesized by 0.01 M $[Co(NH_3)_5(H_2O)]Cl_3$ are composed of about 10 nm-thick single-crystalline nanosheets with the averaged diameter of about 120 nm. Based on the evidence of electron images and the structural characteristics, the formation mechanism of sphere-structure heterogenite has been proposed as a coordination self-assembly process. The coordination self-assembly mechanism is essential to controllable synthesis of nanostructure material since it is based on oriented growth and self-assembly. To the best of our knowledge, this is the first synthesis of such kind of uniform β-CoOOH nanospheres under ultrasonic conditions through coordination self-assembly of heterogenite nanosheets. Our experimental method provides a simple and facile route for the preparation of the heterogenite nanostructures, which may have important application in the field of Ni-MH cells due to the uniform shape and ordered self-assembly of heterogenite nanosheets. Furthermore, the simple ultrasonic-assisted process can be widely applied in inorganic nanomaterials synthesis with well-defined geometries and unique functionalities.

Acknowledgments This work was supported by the Natural Science Fund Council of China (NSFC, No. 20331010).

References

1. N. Bowden, A. Terfort, J. Carbeck, G.M. Whitesides, Science **276**, 233 (1997)
2. D.H. Gracias, J. Tien, T.L. Breen, C. Hsu, G.M. Whitesides, Science **289**, 1170 (2000)
3. L. Hashemi, M. Hosseinifard, V. Amani, A. Morsali, J. Inorg. Organomet. Polym. **23**, 519 (2013)
4. Z.P. Chen, A.Q.Y. Zhang, N. Gu, Curr. Appl. Phys. **10**, 967 (2010)
5. Y. Hanifehpour, B. Mirtamizdoust, S.W. Joo, J. Inorg. Organomet. Polym. **22**, 952 (2012)
6. J.C. Love, A.R. Urbach, M.G. Prentiss, G.M. Whitesides, J. Am. Chem. Soc. **125**, 12696 (2003)
7. K.P. Velikov, C.G. Christova, R.P.A. Dullens, A. Blaaderen, Science **296**, 106 (2002)
8. M.J.S. Fard, A. Morsali, J. Inorg. Organomet. Polym. **20**, 727 (2010)
9. M.C. Brandes, L. Kovarik, M.K. Miller, M.J. Mills, J. Mater. Sci. **47**, 3913 (2012)
10. X.H. Liu, R.Z. Ma, Y. Bando, T. Sasaki, Angew. Chem. Int. Ed. **49**, 8253 (2010)
11. C.H. Chen, S.F. Abbas, A. Morey, S. Sithambaram, L.P. Oxus, H.F. Garces, W.A. Hines, S.L. Suib, Adv. Mater. **20**, 1205 (2008)
12. J.H. Yang, T. Sasaki, Chem. Mater. **20**, 2049 (2008)
13. J.C. Myers, R.L. Penn, Mater. Res. Bull. **46**, 649 (2011)
14. G.M. Whitesides, B. Grzybowski, Science **295**, 2418 (2002)
15. H. Colfen, S. Mann, Angew. Chem. Int. Ed. **42**, 2350 (2003)
16. J. Yuan, K. Laubemds, Q. Zhang, S.L. Suib, J. Am. Chem. Soc. **125**, 4966 (2003)
17. A. Dong, N. Ren, Y. Tang, Y. Wang, Y. Zhang, W. Hua, Z. Gao, J. Am. Chem. Soc. **125**, 4976 (2003)
18. A.D. Dinsmore, M.F. Hsu, M.G. Nikolaides, M. Marquez, A.R. Bausch, D.A. Weitz, Science **298**, 1006 (2002)
19. F. Caruso, R.A. Caruso, H. Mohwald, Science **282**, 1111 (1998)
20. D. Wang, R.A. Caruso, F. Caruso, Chem. Mater. **13**, 364 (2001)
21. K.M. Kulinowski, V. Harsha, V.L. Colvin, Adv. Mater. **12**, 833 (2000)
22. S. Park, J.H. Lim, S.W. Chung, C.A. Mirkin, Science **303**, 348 (2004)
23. P. Poizot, S. Laruelle, S. Grugeon, L. Dupont, J.M. Tarascon, Nature **407**, 496 (2000)
24. A.K. Sood, J. Appl. Electrochem. **16**, 274 (1986)
25. M. Oshitani, H. Yufu, K. Takashima, S. Tsuji, Y. Matsumaru, J. Electrochem. Soc. **136**, 1590 (1989)
26. R.D. Armstrong, G.W. Griggs, E.A. Charles, J. Appl. Electrochem. **18**, 215 (1988)

27. F. Barde′, M.R. Palacin, B. Beaudoin, A. Delahaye-Vidal, J.M. Tarascon, J. Phys. Chem. B **105**, 4690 (2001)
28. Y.C. Zhu, H.L. Li, Y. Koltypin, A. Gedanken, J. Mater. Chem. **12**, 729 (2002)
29. A. Lecerf, Y. Cudennec, Mater. Res. Bull. **29**, 1255 (1994)
30. W.K. Hu, X.P. Gao, M.M. Geng, Z.X. Gong, D. Noresù, J. Phys. Chem. B **109**, 5392 (2005)
31. B.Y. Geng, F.M. Zhan, H. Jiang, Z.J. Xing, C.H. Fang, Cryst. Growth Des. **8**, 3497 (2008)
32. C.H. Lu, L.M. Qi, J.H. Yang, D.Y. Zhang, N.Z. Wu, J.M. Ma, J. Phys. Chem. B **108**, 17825 (2004)
33. B. Liu, H.C. Zeng, J. Am. Chem. Soc. **126**, 8124 (2004)
34. R.L. Penn, G. Oskam, T.J. Strathmann, A.T. Ston, D.R. Veblen, J. Phys. Chem. B **105**, 2177 (2001)
35. X.G. Wen, W.X. Zhang, S.H. Yang, J. Phys. Chem. B **108**, 5200 (2004)
36. E.B. Flint, K.S. Suslick, Science **253**, 1397 (1991)
37. L.P. Jiang, S. Xu, J.M. Zhu, J.R. Zhang, J.J. Zhu, H.Y. Chen, Inorg. Chem. **43**, 5877 (2004)
38. X.F. Qiu, Y.B. Lou, A. Samia, A. Devadoss, J.D. Burgess, S. Dayal, C. Burda, Angew. Chem. Int. Ed. **44**, 2 (2005)